Nonlinear Disturbance Observer Based Control of a 7DoF Exoskeleton Robot for Arm Movements

HOUDA BARBOUCH
Université Tunis Elmanar
École Natinale d'Ingénieurs de Tunis ENIT
Laboratoire RISC
BP,37 le Belvédère,1002Tunis
TUNISIA
barbouchhouda@yahoo.fr

ABDERRAOUF KHEMIRI
Université Tunis Elmanar
École Natinale d'Ingénieurs de Tunis ENIT
Laboratoire RISC
BP,37 le Belvédère,1002 Tunis
TUNISIA
khemiri.abderraouf@yahoo.fr

NAHLA KHRAIEF
Université Tunis Elmanar
École Natinale d'Ingénieurs de Tunis ENIT
Laboratoire RISC
BP,37 le Belvédère,1002 Tunis
TUNISIA
khraiefnahla@yahoo.fr

SAFYA BELGHITH
Université Tunis Elmanar
École Natinale d'Ingénieurs de Tunis ENIT
Laboratoire RISC
BP,37 le Belvédère,1002Tunis
TUNISIA
safyabelghith@yahoo.fr

Abstract: This paper focuses on the application of a disturbance observer control of an exoskeleton upper-extremity. In order to achieve this target, arm two steps were executed; first of all, a prototype of the exoskeleton robot has been designed using Solidworks software, after its dynamic model has been accomplished. Then, the development of non linear controller (Computed Torque Control) was performed. Finally, to the application of a disturbance observer in the control, we have used the Lyapunov method to estimate the external disturbance about the device.

Key–Words: Exoskeleton robot, rehabilitation, physical disability, Computed Torque Control, Nonlinear Disturbance Observer, External disturbance, Lyapunov method. LaTeX

1 Introduction

The partial or the full loss of motor human limbs is known especially of the elderly people as it may occur due a stroke or sports injuries, occupational injuries, or trauma and spinal cord injuries..

In recent decades, an enormous increase has been presented in the number of such cases. But the duration of treatment becames longer.In order to improve the quality of therapies, including intensity, robotics has made its appearance quite naturally in this area of rehabilitation as an evolution of existing mechanical devices. In this context of neuro-motor rehabilitation robotics upper limb that the researchers have developed a wide of exoskeleton systems. These devices are characterized by the number of degrees of freedom, joints with which they are destined to interact(Shoulder, Elbow, Wrist, Fingers), the nature of their actuator (electric, hydraulic, pneumatic...) and the technology power transmission (gears, cables, rods...). Among these different devices may be found: MGA (Maryland Georgetown-Army) Exoskeleton [**?**] [**?**] is a robotic arm with five degrees of freedom dedicated to the rehabilitation of pathological shoulder. This exoskeleton arm will evaluate strength, speed and range of motion. ARMin I, II and III [**?**][**?**] is an exoskeleton with six degrees of freedom and equipped by positional force sensors. Also, it's equipped by a multimodal display system (visual and audio feedback). The ARMin enables us to offer a virtual immersion for the limb to make simple games or ADL (Activities of Daily Living) of the patient. CADEN-7 (Washington University) Exoskeleton [**?**][**?**][**?**] was designed by a team from the University of Washington Which has seven degrees of freedom. They were interested in the problems of singularities. The device and the patient's limb are connected via various force sensors to allow the use of force control. In the aim of obtaining sufficient transparency, the team added EMG signals to the control. Soft-Actuated Exoskeleton [**?**][**?**] is an exoskeleton with seven degrees of freedom. This latter is equipped by pneumatic muscles, that moves the seven active joints, to control the stiffness of each joint as well as to provide a smoother interaction ensuring safety to the user. Finally, ETS-MARSE [**?**][**?**], is a lightweight robot with seven DoFs, it controls all the joints of the upper limb. This robot has a optimal ratio of power / weight and is able to compensate the gravity efficiently.

This article deals with the modeling,the control and applaying a disturbance observer based on Lyapunov method of an exoskeleton upper-extremity with seven degrees of freedom.

This paper is organized as follows: Section 2 deals with the Human arm anatomy. Section 3 deals with two points: First point describes the mechanical modeling of the proposed prototype. Second point

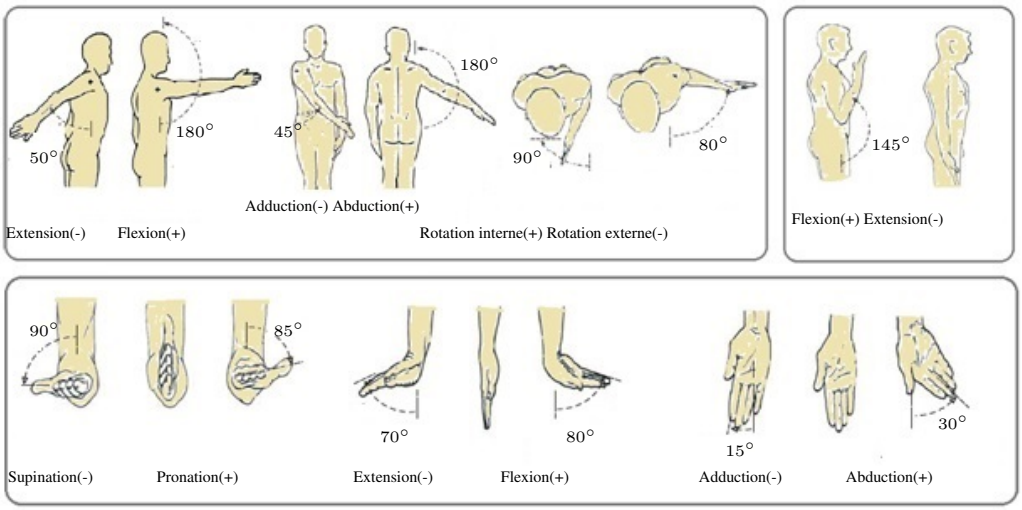

Figure 1: The seven basic degrees of freedom of the arm. Copied from[**?**]

presents the kinematic and dynamic models of the exoskeleton which will be used to control this device by applying the Computed torque control. Section 4 is dedicated to the description of the disturbance observer based on Lyapunov method. Section 5 reports the results of the simulation. Finally, a brief conclusion resume our main contributions as well as the perspectives of this project.

2 Human Arm Anatomy

The human upper limb anatomy can be represented as a set of three rigid bodies; the arm, the forearm and the hand. These bodies are interconnected by three complex articulations; the shoulder, the elbow and the wrist.
The shoulder is the proximal joint of the limb; it has three degrees of freedom (DoF) (flexion/extension, adduction/abduction and externel/internel rotation).
The elbow is the intermediate joint of the limb; it has only one degree of freedom (DoF) (flexion/extension).
And finally the wrist is the distal joint of the limb; it has three degrees of freedom (DoF) (pronation/supination, flexion/extension and adduction/abduction).
These articular motions and its workspace are shown in Fig.1

3 Modeling and Control of the Exoskeleton Upper limb

This section describes the modeling and control of the upper limb exoskeleton. In section 3.1. a mechanical structure of the robot has been developed, after that section 3.2. presents the kinemtic and dynamic modeling. After description of the modeling, different controllers have been developed in the section 3.3.

3.1 Mechanical structure

In our research we have based on the mechanical struture of the robotic arm ETS-MARSE[1], the last was designed to be worn on the right upper-limb as shown in Fig.2 Left. This robot is a redundant kinematic chain with seven revolute joints; each of them is controlled by an actuator. Its kinematic structure is a simplified model of the kinematic structure of a human arm.
By the use of Solidworks software, we have designed a identical prototype of ETS-MARSE shown in Fig.2 right.

3.2 Modeling of the exoskeleton

In order to achieve a compliant controller for the exoskeleton, it is necessary to determine the kinematic and dynamic models.

3.2.1 Kinematic model:

Modified Denavit-Hartenberg has been used to describe the geometry and morphology of the robot[**?**]. By applying this convention on our prototype, the seven joint axes of exoskeleton upper-limb are depicted in Fig 3. The geometric parameters of the

[1]MARSE: "Motion Assistive Robotic Exoskeleton for Superior Extremety" which was develped by a team from ETS (École de Technologie Supérieure of CANADA) www.etsmtl.ca

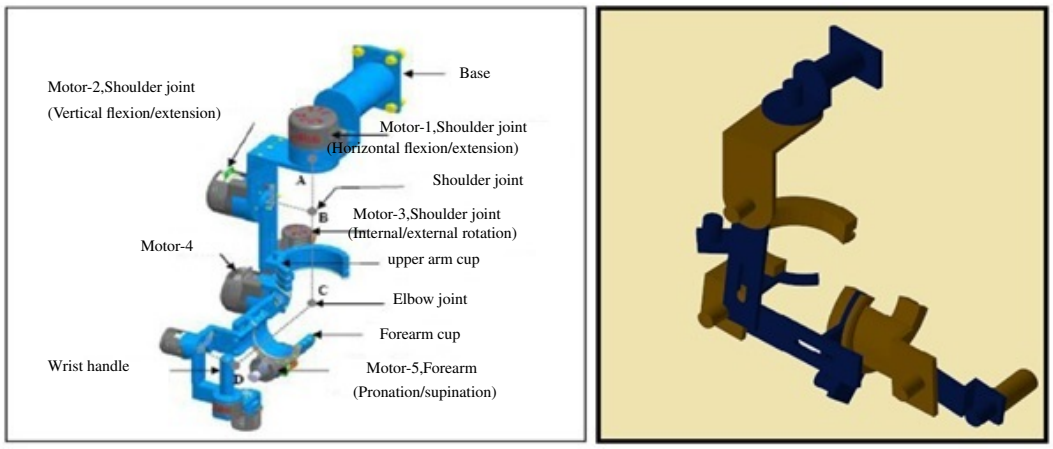

Figure 2: Mechanical model:(a)ETS-MARSE. Copied from [**?**], (b) Our prototype

robot have been shown in Table 5. The model shown in Fig 3 depicts the joint axes of rotation of human arm, where joints 1, 2 and 3 together constitute the glen-humeral joint, commonly known as the shoulder joint: Joint 1 corresponds to abduction/adduction movement, joint 2 to flexion/extension movement and joint 3 to internal/external rotation movement. The joint 4 corresponds to flexion/extension of the elbow, and finally, the last three joints 5, 6 and 7 together intersect at point known as the wrist joint, they correspond successively to pronation/supination, abduction/adduction and flexion/extension.

Articulations	a_{i-1}	d_i	θ_i	α_{i-1}
1	0	d_e	θ_1	0
2	0	0	θ_2	$-\frac{\Pi}{2}$
3	0	d_c	θ_3	$\frac{\Pi}{2}$
4	0	0	θ_4	$-\frac{\Pi}{2}$
5	0	d_p	θ_5	$\frac{\Pi}{2}$
6	0	0	θ_6	$-\frac{\Pi}{2}$
7	0	0	θ_7	$-\frac{\Pi}{2}$

Table 1: Geometric parameters by Modified Denahvit-Hartenberg

With respect the general form of link transformation that relates frame (i) relative to the frame (i-1) is the following:[**?**]

$$ {}^{i-1}_{i}T = \begin{bmatrix} \cos q_i & -\sin q_i & 0 & a_{i-1} \\ \sin q_i \times \cos\alpha_{i-1} & \cos q_i \times \cos\alpha_{i-1} & -\sin\alpha_{i-1} & -d_i \times \sin\alpha_{i-1} \\ \sin q_i \times \sin\alpha_{i-1} & \cos q_i \times \sin\alpha_{i-1} & \cos\alpha_{i-1} & -d_i \times \cos\alpha_{i-1} \\ 0 & 0 & 0 & 1 \end{bmatrix} \quad (1) $$

Using equation (1) and table 5, we obtained the following seven homogeneous transformation matrix:

$$ {}^{0}_{1}T = \begin{bmatrix} \cos q_1 & -\sin q_1 & 0 & 0 \\ \sin q_1 & \cos q_1 & 0 & 0 \\ 0 & 0 & 1 & d_e \\ 0 & 0 & 0 & 1 \end{bmatrix} $$

$$ {}^{1}_{2}T = \begin{bmatrix} \cos q_2 & -\sin q_2 & 0 & 0 \\ 0 & 0 & 1 & 0 \\ -\sin q_2 & -\cos q_2 & 0 & 0 \\ 0 & 0 & 0 & 1 \end{bmatrix} $$

$$ {}^{2}_{3}T = \begin{bmatrix} \cos q_3 & -\sin q_3 & 0 & 0 \\ 0 & 0 & -1 & -d_c \\ \sin q_3 & \cos q_3 & 0 & 0 \\ 0 & 0 & 0 & 1 \end{bmatrix} $$

$$ {}^{3}_{4}T = \begin{bmatrix} \cos q_4 & -\sin q_4 & 0 & 0 \\ 0 & 0 & 1 & 0 \\ -\sin q_4 & -\cos q_4 & 0 & 0 \\ 0 & 0 & 0 & 1 \end{bmatrix} $$

$$ {}^{4}_{5}T = \begin{bmatrix} \cos q_5 & -\sin q_5 & 0 & 0 \\ 0 & 0 & -1 & -d_p \\ \sin q_5 & \cos q_5 & 0 & 0 \\ 0 & 0 & 0 & 1 \end{bmatrix} $$

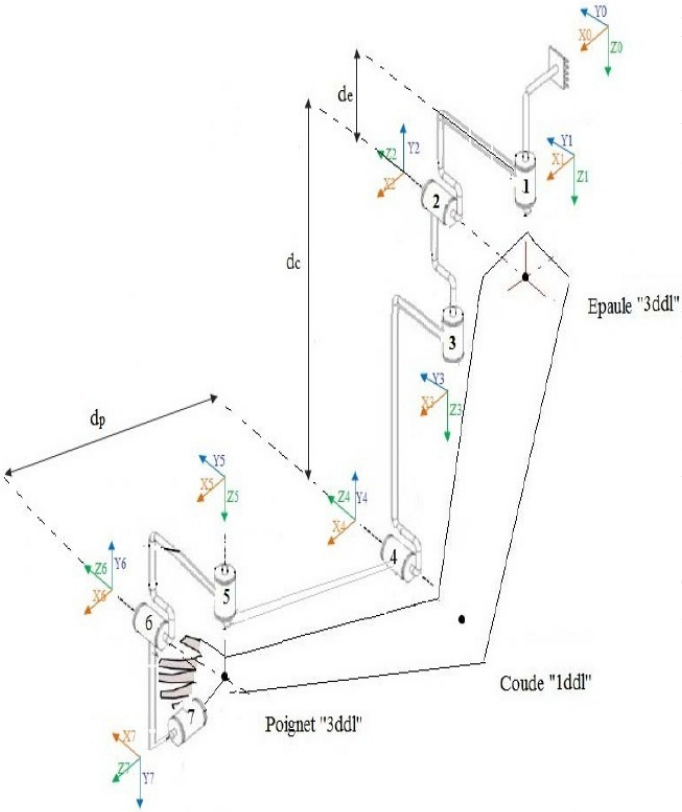

Figure 3: Joint axes of rotation by Modified Denavit-Hartenberg.

$$ {}^{5}_{6}T = \begin{bmatrix} \cos q_6 & -\sin q_6 & 0 & 0 \\ 0 & 0 & 1 & 0 \\ -\sin q_6 & -\cos q_6 & 0 & 0 \\ 0 & 0 & 0 & 1 \end{bmatrix} $$

$$ {}^{6}_{7}T = \begin{bmatrix} \cos q_7 & -\sin q_7 & 0 & 0 \\ 0 & 0 & 1 & 0 \\ -\sin q_7 & -\cos q_7 & 0 & 0 \\ 0 & 0 & 0 & 1 \end{bmatrix} \quad (2) $$

The forwords kinematics results through the homogenous transformation matrix ${}^{0}_{7}T$ that relates frame (7) to frame (0). For that, the following operation is performed:

$$ {}^{0}_{7}T = {}^{0}_{1}T \times {}^{1}_{2}T \times {}^{2}_{3}T \times {}^{3}_{4}T \times {}^{4}_{5}T \times {}^{5}_{6}T \times {}^{6}_{7}T \quad (3) $$

3.2.2 Dynamic model

The dynamic behavior of the exoskeleton has been obtained using Lagrangian method and can be expressed by the following equation:

$$ M(q)\ddot{q} + N(q,\dot{q})\dot{q} + G(q) = \tau \quad (4) $$

Where, M(q) $\in$ $R^{7\times7}$: is the inertia matrix, N(q,$\dot{q}$)$\in$ $R^{7\times7}$: is the coriolis/centrifugal matrix, G(q)$\in$ $R^{7\times1}$: is the gravity vector, τ $\in$ $R^{7\times1}$: is the generalized torques vector, and (q,$\dot{q}$,$\ddot{q}$): represent the joint position, velocity and acceleration vectors created by the motion generator.

3.3 Controller design

In this section, we propose to use the nonlinear control law called "Computed Torque Control". Note that, we added unknown inputs (External disturbances) in the dynamic behavior of the exoskeleton, so that the equation (4) becomes as follows:

$$ M(q)\ddot{q} + N(q,\dot{q})\dot{q} + G(q) = \tau + \delta_{ext} \quad (5) $$

This control type allows tracking trajectory of the developed model. Whether the following control law:

$$ \tau = \alpha \times \tau' + \beta \quad (6) $$

$$ \begin{cases} \alpha = M(q), \\ \beta = N(q,\dot{q})\dot{q} + G(q) - \delta_{ext}, \\ \tau' = \ddot{q} \end{cases} $$

From relation (5) and (6), we may write,

$$ M(q)\tau' + N(q,\dot{q})\dot{q} + G(q) = \tau + \delta_{ext} \quad (7) $$

The general layout of the computed torque control is depicted in Fig4.:

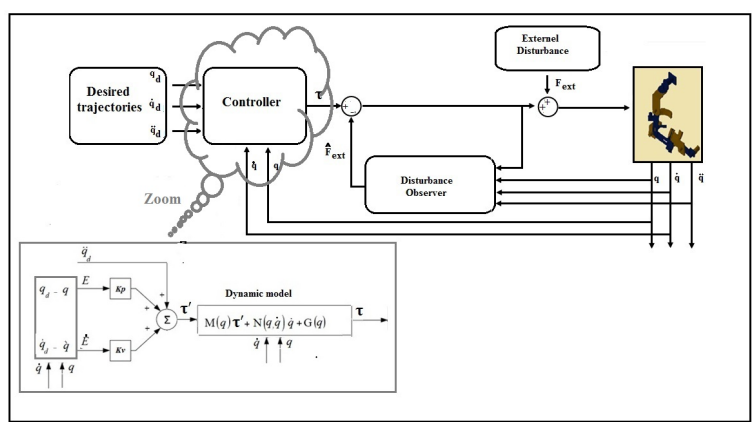

Figure 4: Schematic diagram of the computed torque control [?].

From this schematic (Fig4) the control law can be written as follows:

$$ M(q)(\ddot{q}_d + K_p E + K_v \dot{E}) + N(q,\dot{q})\dot{q} + G(q) = \tau + \delta_{ext} \quad (8) $$

Where;

$$\begin{cases} E = (q_d - q) \\ \dot{E} = (\dot{q}_d - \dot{q}) \\ \ddot{E} = (\ddot{q}_d - \ddot{q}) \end{cases}$$

K_p,K_v: Are the gain matrices, they are diagonal and positive definite.
q_d, $\dot{q}_d$ and $\ddot{q}_d$ are the desired position, velocity and acceleration respectively.
For the system to be stable it is necessary that the following equation is verified:

$$\ddot{E} + K_v\dot{E} + K_pE = 0 \tag{9}$$

4 Observer

In this section, we design an observer based on the Lyapunov method that will estimate the external disturbances exerted on the robot to ensure a rapid convergence towards zero error. The general lay out of the disturbance observer applied in the control of an exoskeleton robot is depicted in Fig 5.:

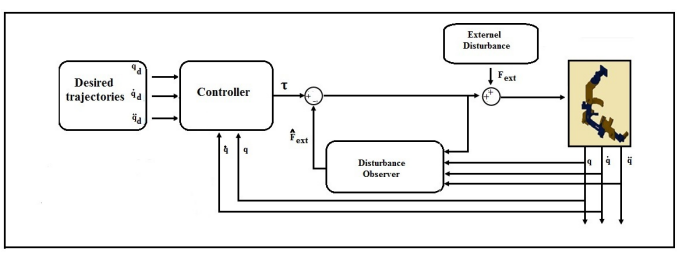

Figure 5: The structure of disturbance observer.

4.1 Nonlinear Disturbance Observer

From the equation (5), the disturbance force can be written as follows:

$$\delta_{ext} = M(q)\ddot{q} + N(q,\dot{q})\dot{q} + G(q) - \tau \tag{10}$$

Thus, the Disturbance Observer can be proposed as follows:

$$\dot{\hat{\delta}}_{ext} = -L(q,\dot{q})\hat{\delta}_{ext} + L(q,\dot{q})(M(q)\ddot{q} + N(q,\dot{q})\dot{q} + G(q) - \tau) \tag{11}$$

Where, $L(q,\dot{q}) \in R^{7\times7}$ is a matrix chosen in such a way that the dynamic of the error is asymptotically stable. Since we don't have prior information about the derivative of F_{ext}, we assume that it varies in a manner very low and slow in comparison to the dynamics of the observer.

$$\dot{\delta}_{ext} = 0 \tag{12}$$

We can define the difference between the actual effort exerted by the patient and the disturbance estimated by the Lyapunov-based nonlinear disturbance observer as an error of observation:

$$e = \delta_{ext} - \hat{\delta}_{ext} \tag{13}$$

By combining (11) and (13), we get:

$$\dot{e} = \dot{\delta}_{ext} - \dot{\hat{\delta}}_{ext} = -L(q,\dot{q})(\delta_{ext} - \hat{\delta}_{ext}) = -L(q,\dot{q})e \tag{14}$$

This allows us to deduce the following differential equation:

$$\dot{e} + L(q,\dot{q})e = 0 \tag{15}$$

According to the equation (11), it's necessary to calculate the acceleration $\ddot{q}$ to realize the disturbance observer, but in robotic applications it's hard to measure the acceleration. For that, we have defined a new variable ψ such that:

$$\psi = \hat{\delta}_{ext} - p(\dot{q}) \tag{16}$$

So;

$$\dot{\hat{\delta}}_{ext} = \dot{\psi} - \frac{\delta p}{\delta \dot{q}}\ddot{q} \tag{17}$$

Replacing (16) and (17) in (11), we obtain:

$$\dot{\psi} - \frac{\delta p}{\delta \dot{q}}\ddot{q} = -L(q,\dot{q})(\psi + p(\dot{q})) + L(q,\dot{q})(M(q)\ddot{q} + N(q,\dot{q})\dot{q} + G(q) - \tau \tag{18}$$

Defining $\frac{\delta p}{\delta \dot{q}}$ as:

$$\frac{\delta p}{\delta \dot{q}} = L(q,\dot{q})M(q) \tag{19}$$

The equation (18) can be written as follows:

$$\dot{\psi} = -L(q,\dot{q})\psi + L(q,\dot{q})(N(q,\dot{q})\dot{q} + G(q) - \tau + p(\dot{q})) \tag{20}$$

So:

$$\hat{\delta}_{ext} = \psi + p(\dot{q}) \tag{21}$$

4.2 Stability Analysis

The design parameters L and p defined in the equation (20) are dependent and related to each other according to the equation (18). Also, they are chosen such that dynamics of the observation error is asymptotically stable. Next, we propose a value for p based on

the joint velocities to ensure the stability of the disturbance observer. Whether defined as:

$$p(\dot{q}) = c.\begin{bmatrix} \dot{q}_1 & 0 & \dots & 0 \\ 0 & \dot{q}_2 & \ddots & \vdots \\ \vdots & \ddots & \ddots & 0 \\ 0 & \dots & 0 & \dot{q}_7 \end{bmatrix} \tag{22}$$

As all the joint velocities are determined. In this case, the asymptotical stability given by (15) will be guaranteed that only the choice of the parameter c. If we drift p with respect to $\dot{q}$ then we obtain as bellows:

$$\frac{\delta p}{\delta \dot{q}} = c.\begin{bmatrix} 1 & 0 & \dots & 0 \\ 0 & 1 & \ddots & \vdots \\ \vdots & \ddots & \ddots & 0 \\ 0 & \dots & 0 & 1 \end{bmatrix} \tag{23}$$

Whether:

$$C = c. * I_{7*7} \tag{24}$$

In applying the equation (22) in the equation (18), this leads to the following result:

$$L(q, \dot{q}) = \frac{\delta p}{\delta \dot{q}} M^{-1}(q) = C.M^{-1}(q) \tag{25}$$

We desire to realize a disturbance observer, with its error dynamics is described by:

$$\dot{e} + C.M^{-1}(q).e = 0 \tag{26}$$

Where, C is a constant, diagonal and positive definite matrix. Then, the Lyapunov function for this observer can be summed up by:

$$V(e, q) = e^T.M(q).e \tag{27}$$

The time derivative of the previous function can be written as:

$$\frac{\delta V(e,q)}{\delta t} = \frac{\delta V(e,q)}{\delta e}\dot{e} + \frac{\delta V(e,q)}{\delta q}\dot{q} \tag{28}$$

Using (12) and (20):

$$\begin{cases} \frac{\delta V}{\delta e}\dot{e} = -2e^T.M(q).C.M^{-1}(q).e \\ \frac{\delta V}{\delta q}\dot{q} = e^T.\frac{\delta M(q)}{\delta q}\dot{q}.e \end{cases}$$

Using the adaptation laws in (17) and the external disturbance δ_{ext}, the time derivative of V becomes:

$$\frac{\delta V(e,q)}{\delta t} = \frac{-1}{2}e^T.P.e \tag{29}$$

Now, we have to prove that $\frac{\delta V(e,q)}{\delta t} < 0$. For this, P must be symmetric and positive definite matrix [**?**]. According to the last condition of the time derivative of V and the equations (11) and (12), we can conclude that the looped system is stable [**?**].

5 Simulation and results:

This section aims to present the simulation results achieved in Matlab/Simulink by doing a comparative study on some exercises to identify the performance of an observer in the control of an exoskeleton robot. The following expression depicts the law of observation applied in the computed torque control:

$$\hat{\dot{\delta}}_{ext} = C.(\ddot{q}_d - \ddot{q}) + C.K_v.(\dot{q}_d - \dot{q}) + C.K_p.(q_d - q) \tag{30}$$

The simulations are performed for two cases, the first is a control without disturbance observer and the second is a control with disturbance observer. The Fig **??** and the Fig5 depict the angular position simulations and the angular velocity respectively of joint 3 (internal/external rotation movement of shoulder) and joint 4 (flexion/extension of elbow). We note that the proposed control ensures the desired trajectory tracking properly for both the simulation. nevertheless, the convergence time to zero by the control with DO is faster than that given by the control without DO. We can see that there's no big difference in both cases, this is shown in the figures of error curves Fig 5 and Fig 5 that screen the deviation between the desired and measured trajectories for the two cases.
These simulation results, show clearly that the proposed observer provides in a finite time a asymptotic convergence of observation errors to zero which means a rapid convergence of real states to the estimate states of system . Furthermore, they show that the proposed control law ensures the desired trajectory tracking.

6 Conclusion and future works

An exoskeleton robot with 7Dofs has been presented in first step. Then,the kinematic and dynamic model of the proposed prototype has performed. After, the nonlinear Computed Torque Control has applied. Finally, a comparative study was conducted between the control with and without Nonlinear Disturbance Observer(NDO) based Lyapunov method. This study, shown that the performance and effectiveness of the NDO in the proposed control. Future works will include the experimental validation phase for these works using the FES signals as a first step. After, the use of other control techniques as sliding mode control or adaptive control. Furthermore, the application of other NDO method as Kalman Filter or sliding mode observer.

References:

[1] C. Carignan, M. Naylor, S. Roderick, Controlling shoulder impedancein a rehabilitation arm exoskeleton, in: Robotics and Automation, 2008.ICRA 2008. IEEE International Conference on, YEAR = 2008, pages: 2453 - 2458, address : Pasadena, CA, month = May, publisher :IEEE,.

[2] N. Jarrasse, J. Robertson, P. Garrec, J. Paik, Design and acceptability assessment of a new reversible orthosis, in: Intelligent Robots and Sys- tems, 2008. IROS 2008. IEEE/RSJ International Conference on, IEEE, Nice, 2008, pp. 1933 1939.

[3] J. Rosen, J. Perry, N. Manning, S. Burns, The human arm kinematics and dynamics during daily activities - toward a 7 dof upper limb powered exoskeleton, in: Advanced Robotics, 2005. ICAR 05. Proceedings., 12th International Conference on, IEEE, Seattle, WA, 2005, pp. 532 539.

[4] J. Perry, J.C.and Rosen, S. Burns, Exoskeletons for gait assistance and training of the motor-impaired., IEEE, 2007.

[5] Laffranchi, Design of a 7 degree-of-freedom upper-limb powered ex- oskeleton, pp. 805810.

[6] K. Ouimet, Commande dun bras exosquelette sept degr de libert.

[7] M. Rahman, Developpement of an exoskeleton robot for upper-limb rehabilitation, IEEE, Montreal, ON, 2012.

[8] Craig., Introduction to robotics: mechanics and control, 3rd, 2005, p. 400.

[9] M. Rahman, M. Saad, J. Kenne, P. Archambault, Modeling and devel- opment of an exoskeleton robot for rehabilitation of wrist movements, in: Advanced Intelligent Mechatronics (AIM), 2010 IEEE/ASME Inter- national Conference on, IEEE, Montreal, ON, 2010, pp. 25 30.

[10] H. Amin, Nikoobin andReza, Lyapunov-based nonlinear disturbance ob- server for serial n-link robot manipulators, Springer Science + Business Media B.V., Iran, 2008.

[11] K. Reif, F. Sonnemann, R. Unbehauen, An ekf-based nonlinear observer with a prescribed degree of stability, pp. vol. 34, no 9, app 11191123, (1198).

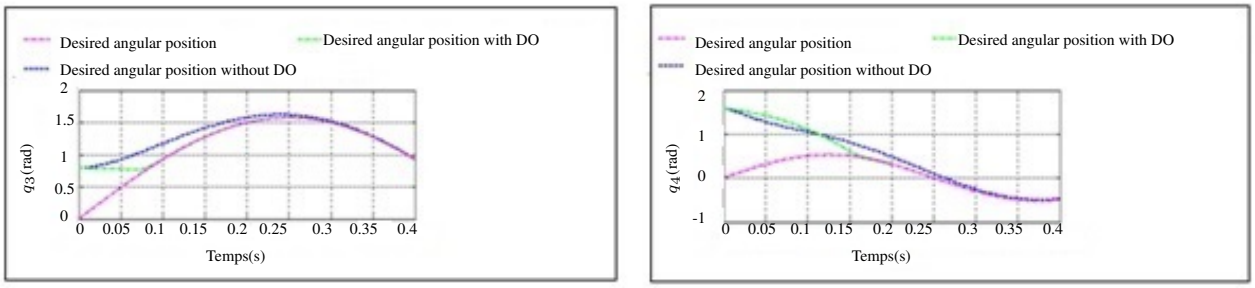

Figure 6:Angular position with and without DO.

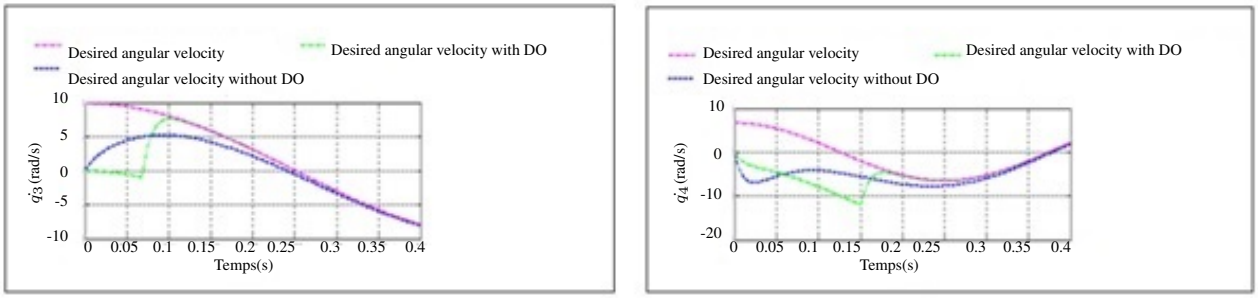

Figure 7:Angular velocity with and without DO.

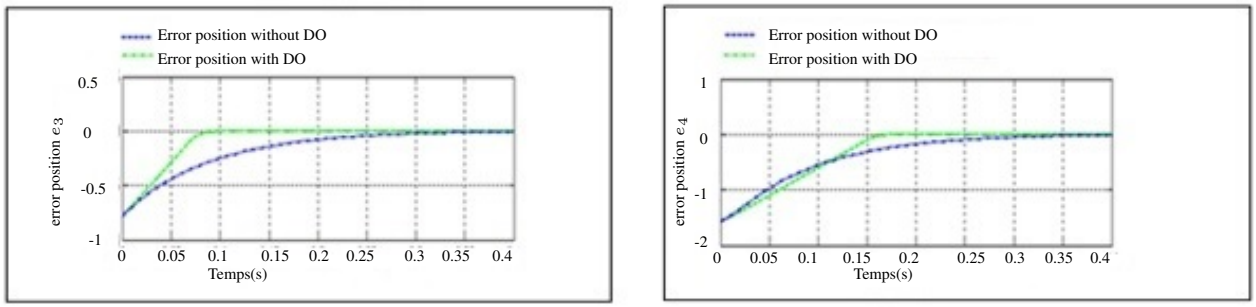

Figure 8:Error position with and without DO.

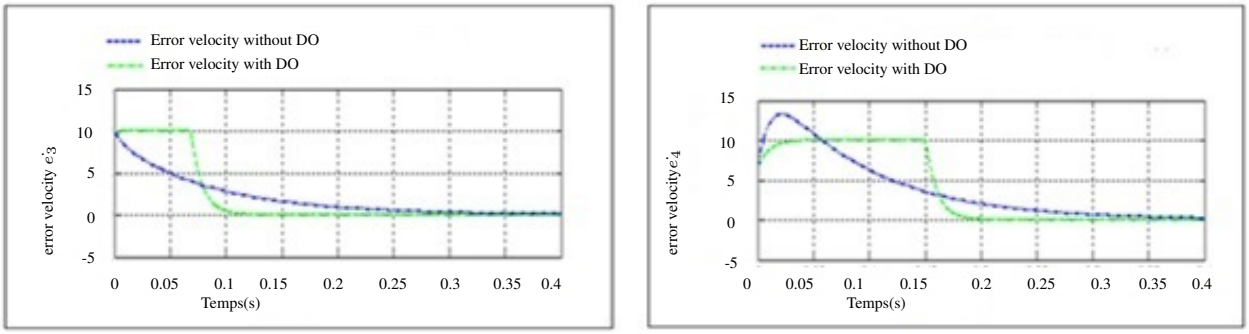

Figure 9:Error velocity with and without DO.